Aquat. Living Resour. 2021, 34, 11

https://doi.org/10.1051/alr/2021011

Aquatic Living Resources
Available online at:
www.alr-journal.org

Perspective Note

The relationship between target strength frequency response and vertical swim velocity: a new approach for fish discrimination

Hikaru Homma* and Ilia Ostrovsky

Israel Oceanographic and Limnological Research, Yigal Allon Kinneret Limnological Laboratory, P.O. Box 447, Migdal 1495000, Israel

Received 20 October 2020 / Accepted 30 April 2021

Handling Editor: Verena Trenkel

Abstract – *In-situ* identification of fish species using acoustic methods is a key issue for fisheries research and ecological applications. We propose a novel approach to fish discrimination based on the relationship between target strength frequency response (TS(*f*)) and vertical swim velocity (VSV), as a proxy of fish body orientation. The measurements were carried out with a wideband echosounder on live fish of five species confined in a net cage. The data show a large dependence of TS(*f*) on VSV. To compare the variability of frequency responses of different fishes, we calculated ΔTS(*f*, VSV) as the difference between the TS(*f*) at given VSV and the TS(*f*) at VSV = 0, i.e. when the fish was swimming horizontally. We demonstrated that the relationships between ΔTS and VSV were similar for fish of the same species but dissimilar for different species. This implies that the acoustic fish discrimination in nature might be performed when the variations of the VSV can be measured from acoustically tracked fish. This can be a promising method for remote fish discrimination, for instance, for fish with diurnal vertical migrations. Further validation of this approach for fish recognition is required.

Keywords: Fish species discrimination / wideband echosounder / target strength / frequency response / vertical swim velocity

1 Introduction

Remote acoustic identification of fish species has been a major issue for fishery management and stock assessment in different marine and freshwater ecosystems. One of the promising methods is to use multiple echosounders to detect species-specific variations of backscattering strengths at different acoustic frequencies (e.g., Gorska et al., 2004; Korneliussen, 2018; Boyra et al., 2019). Recent studies suggest implementing wideband echosounders for species identification, which allow obtaining frequency response of backscattering strength, i.e. the backscattering strength can be presented as a function of acoustic frequency (e.g., Demer et al., 2017; Berges and van Helmond, 2018).

Many fish have gas-bearing swimbladders, which are responsible for the strong backscatter of acoustic waves. The characteristics of the backscattered signal largely depend on the morphology of the swimbladder. The backscattering strength varies with fish body orientation (tilt) due to change of the cross-sectional area of a swimbladder perpendicular to the incident acoustic beam (e.g., Blaxter and Batty, 1990). The variability of fish target strength (TS) with body orientation was demonstrated by *ex-situ* experiments (e.g., Nakken and Olsen, 1977) and by acoustic scattering models (e.g., Kang and Hwang, 2003). Various fish species have different variability of TS depending on body orientation (Benoit-Bird et al., 2003; Gauthier and Horne, 2004). Lundgren and Nielsen (2008) detected the species-characteristic properties of the relationship between wideband frequency response and body orientation based on *ex-situ* measurements on live swimming fish. These authors suggested that the observed backscattering-directivity patterns may be used to discriminate between juvenile gadoids under experimentally controlled conditions.

The main aim of this work is to study the dependence of frequency responses of various fish species on vertical swim velocity (VSV), as a proxy of body orientation, and reveal the species-specific patterns that can be used for remote discrimination between five studied species.

*Corresponding author: hommalight@gmail.com

Table 1. Characteristics of the studied fishes. TS(70, 0) is the TS at 70 kHz and zero vertical swim velocity.

Scientific name (common name)	Abbreviation	Total length (cm)	Weight (g)	TS(70, 0) (dB)	Date of measurements
Sarotherodon galilaeus #1 (Mango tilapia)	*Sg*1	14.0	56	−44.3	18 Nov
Sarotherodon galilaeus #2 (Mango tilapia)	*Sg*2	16.5	88	−45.4	25 Nov
Tilapia zillii (Redbelly tilapia)	*Tz*	20.0	146	−40.0	21 Nov
Oreochromis aureus (Blue tilapia)	*Oa*	26.0	264	−40.1	18 Nov
Mugil cephalus (Flathead grey mullet)	*Mc*	19.0	66	−48.4	24 Dec
Cyprinus carpio #1 (Common carp)	*Cc*1	34.0	583	−37.5	18 Nov
Cyprinus carpio #2 Common carp)	*Cc*2	35.0	628	−38.6	21 Nov

2 Materials and methods

2.1 Cage experiments

The experiments were conducted on five fish species inhabiting Lake Kinneret (Israel) which have commercial values and play important roles in the ecosystem (Ostrovsky et al., 2014). We studied seven individuals of five species (see Tab. 1 for fish species names, specimens, and their abbreviations). Carp have two-chambered "physostomous" swimbladder, which is connected to gut (e.g., Grom, 2015). Tilapias have two-chambered "physoclistous" (closed) swimbladders (e.g., Butler et al., 2017). Mullet have one-chambered physoclistous swimbladder (e.g., Moore, 1970). The fishes ranged 14–35 cm in total length and 56–628 g in weight (Tab. 1). The fishes were provided by the Aquaculture Research Station in Ginosar (the Department of Fisheries and Aquaculture, Israel Ministry of Agriculture and Rural Development). The experiments were carried out in a freshwater pond (~2.3 m depth) of the station.

The acoustic data were collected from live healthy fishes placed in a net cage that was submerged in the pond. The net cage was made of a thin plastic wireframe covered with a 0.12-mm monofilament nylon fishing net. The cage dimensions (length × width × height) were 40 × 30 × 55 cm. The cage was suspended in the water. The top corners of the cage were connected to a 1.5 × 1.5 m plastic frame floating on the water surface; the bottom corners were connected to a metal frame lying on the bottom of the pond. The upper surface of the cage was positioned at 1.4 m below the water surface. A down-looking echosounder transducer was mounted in the middle of the floating frame just above the cage center. The transducer's face was situated at ~0.1 m below the water surface. A single fish was placed in the cage for each trial. The measurements were started in about 5 minutes after fish was placed into the cage and lasted for about 30–40 min. The experiments were conducted between 18 November and 24 December 2018.

The acoustic measurements were carried out with Simrad EK80 wideband echosounder that consisted of the transceiver WBT Tube and the split-beam transducer ES70-7c whose nominal acoustic frequency is 70 kHz. The echosounder allowed collecting wideband acoustic data covering 45–90 kHz. The nominal half-power (3-dB) beamwidth corresponds to 7°. The pulse duration and ping interval were 0.512 ms and 0.4 s, respectively. The echosounder was calibrated using a standard tungsten sphere of 38.1 mm.

2.2 Data processing

The recorded acoustic data were processed by the software Echoview 9 (Echoview Software Pty. Ltd.) to track the fish and compute the frequency responses of their TS. The pulse-compressed wideband backscattering strength (e.g., Chu and Stanton, 1998) with a vertical resolution of <2 cm were used for analyses. The single-target echoes and tracks were detected from the acoustic data by using the single target and fish track detection functions of the Echoview (for more details see Sect. 1 of Supplementary Material, hereafter SM1). The single-target echoes assigned to fish tracks were used for further analyses. To reveal long tracks for the calculation of the fish VSV, the threshold of beam compensation function for the single target detection was set to 17.5 dB. Some echoes from the unwanted objects (i.e., cage wireframe, TS < −70 dB) wrongly assigned to fish tracks were removed manually. For the analyses of the relationships between frequency response and VSV, we used the single-target echoes within 3-dB beam compensation, which is equivalent to 7° nominal beam width.

The frequency response of TS depending on the measured band of acoustic frequencies (f), denoted as TS(f), was calculated by the Echoview using the method suggested by Demer et al. (2017). To assess the TS(f) for each single-target echo, the Echoview defines a section of a vertical profile of the backscattering strength around a single target as the center of the section. The vertical size of the section was set to 0.1 m to avoid possible contamination by signals from unwanted objects. More details about the TS(f) computation methods are presented in SM2. The calculated TS(f) covered the 45–90 kHz range with a resolution of 0.06 kHz. Since TS(f)s show sharp variations near the edges of the measured frequency band (Fig. S1 in SM3), we considered the narrower band of 50–85 kHz for further analysis.

Since direct observations on fish body orientation is usually impossible or difficult during acoustic surveys in nature, VSV was used as a proxy of body orientation of fish taking that fish is tilted upward at positive VSV and downward at negative VSV. The VSVs of fish motion (positive upward) were calculated from the change of target depth with time between the adjacent echoes assigned to each fish track. To increase the accuracy of the VSVs by removing small depth fluctuations, the depth time series of fish tracks were smoothed by using a low-pass filter with a cutoff frequency of 0.5 Hz. It should be noted that fish body orientation could not be monitored directly in our experiments due to high turbidity of the pond water.

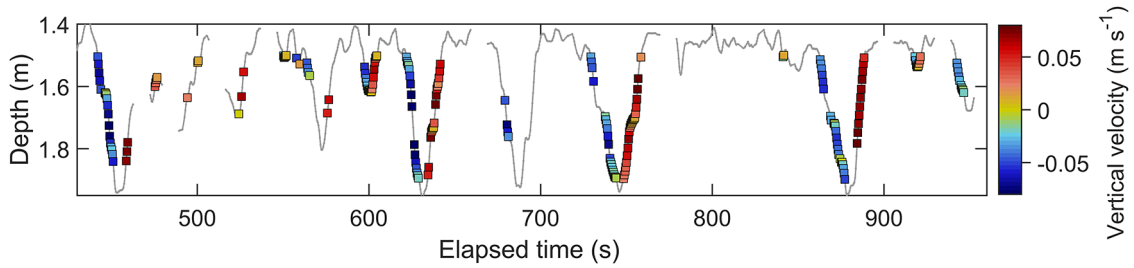

Fig. 1. Example of the tracks of *Sarotherodon galilaeus* #1 (*Sg*1) showing the fish depth location and vertical swim velocity in a cage experiment. Small colored squares represent the echoes satisfying the criteria of the quality control (see SM3). Colors of the squares indicate fish vertical swim velocities (color bar).

The TS(*f*)s with irregular shapes of their curves were excluded from our analyses. The irregular shapes were characterized as exceptionally large TS variation within each TS(*f*) comparatively to the majority of TS(*f*)s obtained from the same individual. Moreover, the TS(*f*)s observed at the top/bottom of the cage (i.e., the fish may have flipped) or during rapid change of the VSV were removed since these could impair the consistency between VSV and fish body orientation in the cage. More details about the quality control are described in SM3.

The obtained TS(*f*)s were averaged over acoustic frequency and time. The 5-kHz moving average of TS(*f*) was assessed for each echo. Further, we calculated the time-averaged TS(*f*) from TS(*f*)s of the echoes within the 2 s centered at each time step. The computation of the average TSs was performed in the linear domain.

2.3 Analyses of target strength frequency response

For the comparison of absolute TS levels between TS(*f*)s, we selected TS at 70 kHz, TS(70), as a measure of the level of each TS(*f*).

To compare the variability of TS(*f*) of fishes with VSV, we calculated ΔTS(*f*, VSV) as the difference between the TS(*f*) at given VSV, TS(*f*, VSV), and the TS(*f*) at VSV = 0, TS(*f*, 0), i.e. when the fish was swimming horizontally. Then,

$$\Delta\mathrm{TS}(f,\mathrm{VSV}) = \mathrm{TS}(f,\mathrm{VSV}) - \mathrm{TS}(f,0) \qquad (1)$$

In practice, for each fish the TS(*f*, 0) was calculated as the average TS(*f*, VSV) of the echoes at which VSVs ranged between −0.01 and 0.01 m s^{-1}. We selected ΔTS at 70 kHz, ΔTS(70, VSV), to compare different fishes. For simplicity, we denote ΔTS(70, VSV) by ΔTS(VSV) unless otherwise stated.

3 Results

The TS(*f*)s of each fish showed large variations in their TS(70) and curve shape with swimming behavior. For instance, the tracks of *Sg*1 indicate that this specimen was swimming up and down in the cage (Fig. 1). These motions were accompanied by large variations in TS(*f*) (Fig. 2). The difference in TS(70) between the lowest and highest TS(*f*) curves exceeded 10 dB. The other specimens exhibited even larger variations in TS(*f*) (see Fig. S5 in SM4). Our measurements did not show any influence of fish position in the cage (fish depth, angles in the acoustic beam) on the TS(70) (see SM5 for more details). In contrast, the TS(*f*) variations were associated with the changes in VSV. For *Sg*1, the TS(70), as well as TSs at other frequencies, tended to increase when the fish was swimming downward and decrease when the fish was swimming upward (Figs. 1 and 2).

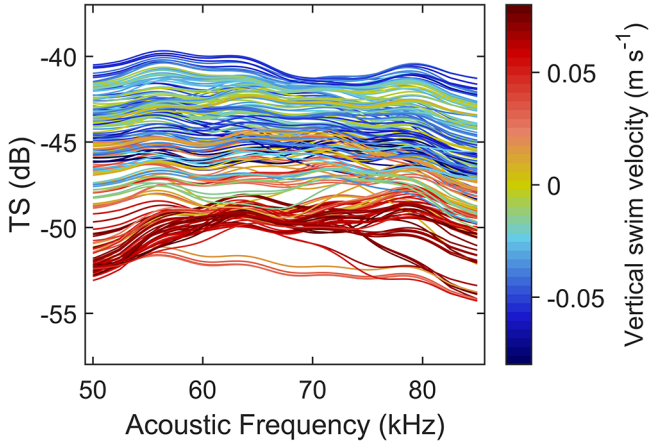

Fig. 2. Target strength frequency responses, TS(*f*), of high-quality echoes (Fig. 1, squares) of *Sg*1. Colors of the lines indicate the vertical swim velocities of fish (color bar). The TS(*f*) curves of the same individual showed variations in shape and TS at 70 kHz (a measure of TS level of each TS(*f*)).

The ΔTS(VSV) of the studied fish are presented in Figure 3. The TS(70, 0) values given in Table 1 were used in equation (1) for calculations of ΔTS(VSV). The ΔTS of *Sg*1 generally increased with decreasing VSV. The ΔTS reached the largest values when VSVs were between −0.05 and −0.03 m s^{-1}. The ΔTSs at other acoustic frequencies showed similar changes with VSV (Fig. S7 in SM6).

Another individual of the same species (*Sg*2) showed a similar tendency of the relationship between ΔTS and VSV to that of *Sg*1. Its ΔTS decreased with increasing VSV (Fig. 3). In contrast, various fish species displayed different behavior of ΔTS change with VSV (Fig. 3). *Mc* showed a generally similar tendency of ΔTS change to those of *Sg1* and *Sg2* but with a notably steeper slope. The ΔTS of *Oa* increased with decreasing VSV and dropped rapidly when VSV decreased below −0.05 m s^{-1}. For *Tz* the ΔTS displayed the maximal

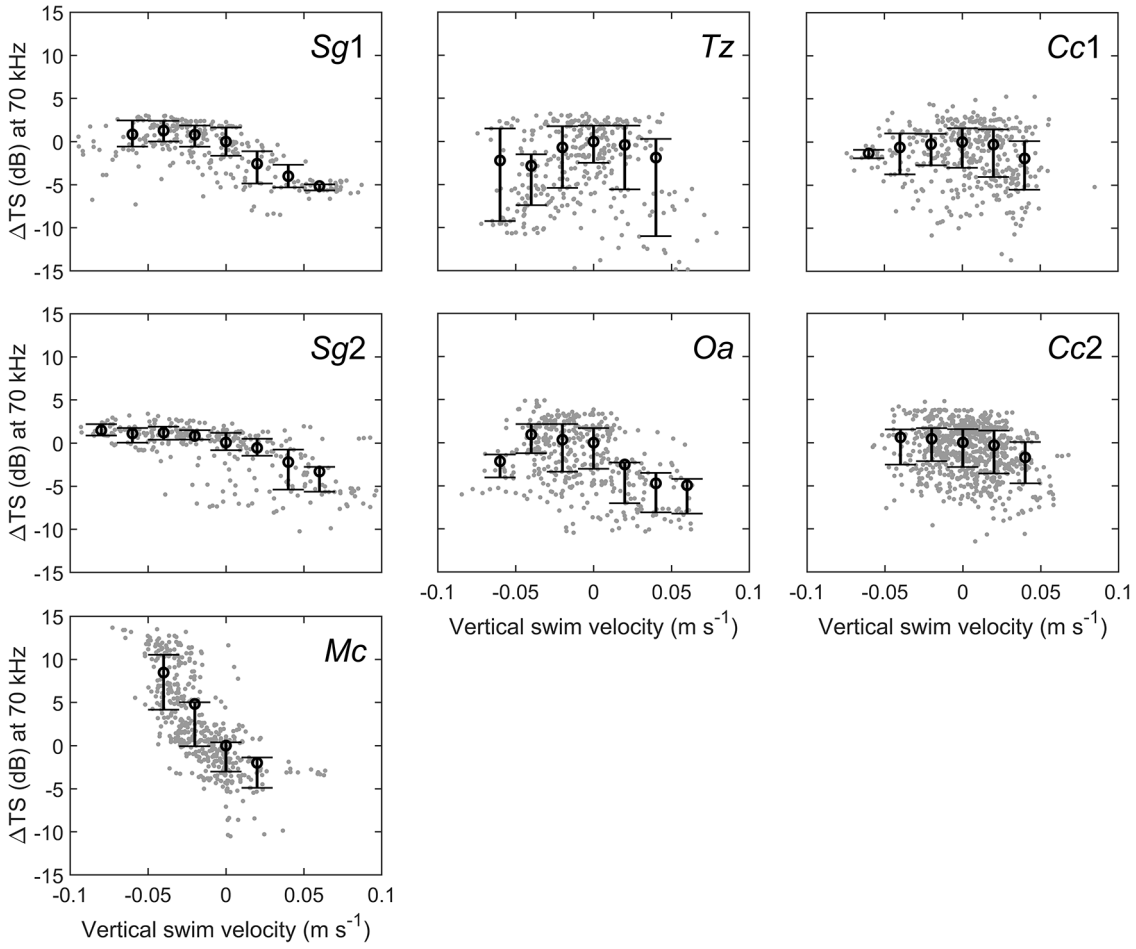

Fig. 3. Relationships between ΔTS (Eq. (1)) at the frequency of 70 kHz and vertical swim velocity, VSV, for studied fishes: *Sg*1, *Sg*2, *Mc*, *Tz*, *Oa*, *Cc*1, and *Cc*2 (see Tab. 1 for species abbreviation). Large empty dots and vertical bars represent the means and 25th–75th percentile ranges of the ΔTS at each 0.02 m s^{-1} VSV bin. The means and 25th–75th percentile ranges are calculated for bins with >14 data points. The changes of ΔTS with VSV reveal different species-characteristic patterns.

values when VSVs were about 0 m s^{-1}. *Cc*1 and *Cc*2 did not show distinct patterns of ΔTS change with VSV.

To clarify the patterns of the ΔTS-VSV relationship for the different species, the mean ΔTS was computed at each 0.02 m s^{-1} VSV bin for each species. The mean characteristic ΔTS-VSV patterns are presented in Figure 4. The ΔTS of *Sg* and *Mc* generally decreased with increasing VSV monotonically within the VSV ranges, while the ΔTS-VSV curves of *Tz*, *Oa*, and *Cc* showed specific ΔTS peaks. *Mc* can be distinguished from *Sg* by notably steeper slope of the ΔTS-VSV relationship. The ΔTS for *Oa* and *Cc* show maxima at negative VSVs, while the maximum of ΔTS for *Tz* is at zero VSV. The ΔTS-VSV curve of *Oa* can be discriminated from that of *Cc* by rapid decrease in ΔTS with VSV between 0 and 0.04 m s^{-1}. Thus, the studied species reveal different patterns of their relationships between ΔTS and VSV.

As a simple use of ΔTS for species discrimination, we examined the differences in mean ΔTSs at specific VSVs between various species pairs. The mean ΔTS(−0.04)s of all species, except the pairs *Oa*-*Sg* and *Oa*-*Cc*, were significantly different from each other ($P < 0.001$, unequal variance *t*-test, e.g., Derrick et al., 2016). The mean ΔTS(0.04) of *Oa* was

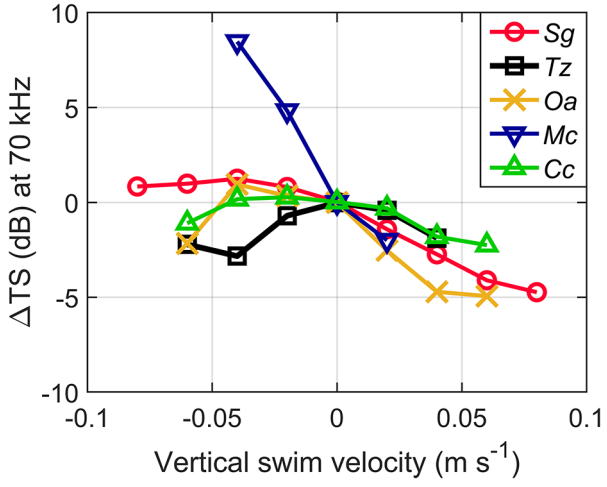

Fig. 4. Comparison of ΔTS-VSV relationships between fish species. Mean ΔTS at the frequency of 70 kHz at each 0.02 m s^{-1} vertical swim velocity (VSV) bin was computed for each studied fish species (see Tab. 1 for species abbreviation) and was plotted against VSV. The pattern of ΔTS versus VSV shows different characteristics by fish species.

significantly different from those of *Sg* and *Cc* ($P < 0.02$ and $P < 0.001$, respectively). The observed statistically significant differences in the ΔTSs between five fish species suggest that the proposed method might be a useful tool for fish discrimination.

4 Discussion

4.1 Vertical swim velocity as a proxy of fish body orientation

The observed variations in ΔTS with VSV agree with the results of other studies showing the dependence of TS on body orientation for fish with swimbladder. For instance, Nakken and Olsen (1977) found that TS of the fish insonified dorsally displayed its maximal value when the fish was tilted downward. In our study, *Sg*, *Mc*, *Cc*, and *Oa* showed the higher ΔTS values for fish swimming downward (Fig. 4). The TS differences between the maximal and minimal values of the same individual exceeded 10 dB (Fig. 2 and Fig. S5 in SM4), which is consistent with the data presented by Nakken and Olsen (1977). Blaxter and Batty (1990) explained this as a result of swimbladders tilting up to the body axis of fish, which lead to the swimbladder axes be normally oriented to acoustic beam when the head tilted down. Similar effect was demonstrated by using the acoustic scattering models that take into account the real morphometric characteristics of fish including the shape and orientation of swimbladder (e.g., Kang and Hwang, 2003). The agreement of our observations with these studies confirms that the VSV measured from acoustic fish tracking portrays fish body orientation: when the VSV is positive, negative, or 0 m s^{-1}, the fish body is tilted up, down, or directed horizontally, respectively.

4.2 Patterns of ΔTS–VSV relationships

The difference in the pattern of ΔTS–VSV relationship between various species observed in this study (Fig. 4) can be associated with species-characteristic shapes of swimbladders and their tilts relative to the dorsal aspect of the fish. This is supported by studies which showed different TS changes with body orientation of various fish species that have different swimbladder shapes, sizes, and orientation angles measured using X-ray images (Benoit-Bird et al., 2003). Gauthier and Horne (2004) also demonstrated the species-specific TS variations with fish body orientation by using the acoustic scattering models that consider the morphometric characteristics of swimbladders of various species. These findings might explain why the patterns of ΔTS–VSV relationships varied depending on fish species in our study (Fig. 4). In fact, despite the similarity of some parameters, such as total lengths of *Tz* and *Mc* or weights of *Sg*1 and *Mc* (Tab. 1), these species showed different ΔTS–VSV patterns (Figs. 3 and 4). The differences in the observed ΔTS–VSV patterns can be attributed to dissimilarity in the swimbladder morphology and orientation, rather than fish size or weight. Notably, the various individuals of the same species (*Sg*1 and *Sg*2; *Cc*1 and *Cc*2) displayed similar patterns of the ΔTS-VSV relationship (Fig. 3) despite their different lengths or weights (Tab. 1). This suggests that the ΔTS–VSV patterns can be species-specific. The significant differences in the observed ΔTSs between species allow implementing a large variety of classification methods to distinguish between the ΔTS–VSV patterns, for instance, discriminant analysis and neural network that have been tested for remote fish separation (e.g., Berges and van Helmond, 2018). Further experiments with a large number of individuals of different size groups and investigations of the swimbladder morphology of the studied species are needed to better determine the species-characteristic patterns of the relationship between ΔTS(f, VSV) and VSV.

Still, the quantitative relationships presented in this study might be biased to some extent due to limited number of measurements, shallow depth of the pond, and a small size of the cage. For instance, a small cage could confine the motions of fish, especially large specimens (e.g., *Cc*1 and *Cc*2), and alter their swimming behavior. This might weaken the consistency between fish VSV and body orientation. The short distance between transducer and backscatterer may cause the near-field effect; however, in our experiments the near-field range was 1.2 m, and the cage was positioned out of the near-field range (see SM7 for more details). Interferences of backscattering signals of fish and cage frame may diminish the quality of the obtained acoustic data. Therefore, in future studies the measurements should be conducted in a deeper location and larger cage to improve the accuracy of the ΔTS-VSV relationships and to widen the ranges of fish sizes and VSVs for the measurements.

Nonetheless, while the shortages mentioned above can affect the accuracy of the measured TS(f), the observed consistencies of the ΔTS–VSV relationships for the same species and the differences for various species suggest that the analysis of the ΔTS–VSV relationships can be an effective approach to discriminate fish in nature when the VSV can be monitored, for instance, for the fish that have diurnal vertical migrations.

Supplementary Material

Table S1. Parameter values used in the fish track detection function of Echoview.

Fig. S1. Example of target strength frequency response, TS(f), at 45 to 90 kHz obtained from *Sarotherodon galilaeus* #1. Vertical dashed lines represent the upper and lower limits of the frequencies used for data analyses. Color bar indicates the vertical swim velocities of the fish for each TS(f).

Fig. S2. Examples of the atypical target strength frequency responses, TS(f)s, of *Sarotherodon galilaeus* #1 with the irregular shapes, i.e., large variations of TS with f that were excluded from the data analyses. Color bar indicates the fish vertical swim velocity for each TS(f).

Fig. S3. Histograms of TS standard deviation calculated for each TS(f) curve and their empirical cumulative distribution function (see Table 1 in the main text for species abbreviations). For each studied fish, the 90th percentile was used as the threshold to exclude the TS(f)s with exceptionally large TS variations.

Fig. S4. Histogram of VSV variance over 5 sec measured from all studied fish. The 95th percentile of the VSV variance

(vertical dashed line) was used as the threshold to remove the data with exceptionally large VSV variance.

Fig. S5. Target strength frequency response, TS(f), from various fishes (see Table 1 in the main text for species abbreviations). The data show large variations in TS at each f. Color bar indicates the fish vertical swim velocity for each TS(f).

Fig. S6. Relationships between TS at 70 kHz and fish positions in the cage: (a) fish depth, (b) major axis angle of the fish in the acoustic beam, and (c) minor axis angle. See Table 1 in the main text for species abbreviations. Large empty dots and vertical bars represent the means and 25th–75th percentile ranges of TS at each (a) 0.05 m depth bin and (b,c) 1° angle bin. The relationships between the TS and fish positions did not show distinct patterns.

Fig. S7. Relationships between ΔTS (Eq. 1 in the main text) and vertical swim velocity at different acoustic frequencies for *Sg*1. Large empty dots and vertical bars represent the means and 25th–75th percentile ranges of ΔTS at each 0.02 m s^{-1} bin. The relationships show close similarities in patterns at various frequencies.

The Supplementary Material is available at https://www.alr-journal.org/10.1051/alr/2021011/olm.

Acknowledgements. We thank S. Kaganovsky for his technical assistance during the cage experiments. We express our gratitude to G. Snovsky (the Ministry of Agriculture and Rural Development of Israel, Fisheries Department) for assistance during the cage experiments and for providing the live healthy fishes. We thank the anonymous reviewers and editor for their careful reading of our manuscript and their useful comments and suggestions. This study was funded by the Ministry of Science and Technology, Israel (3-14470).

References

Benoit-Bird KJ, Au WWL, Kelley CD. 2003. Acoustic backscattering by Hawaiian lutjanid snappers. I. Target strength and swimbladder characteristics. *J Acoust Soc Am* 114: 2757–2766.

Berges BJP, van Helmond ATM. Wageningen Marine Research Report No. C010/18, 2018.

Blaxter JHS, Batty RS. 1990. Swimbladder "behaviour" and target strength. *Rapp P.-v. Réun Cons Int Explor Mer* 189: 233–244.

Boyra G, Moreno G, Orue B, Sobradillo B, Sancristobal I. 2019. *In situ* target strength of bigeye tuna (*Thunnus obesus*) associated with fish aggregating devices. *ICES J Mar Sci* 76: 2446–2458.

Butler JM, Whitlow SM, Gwan AP, Chakrabarty P, Maruska KP. 2017. Swim bladder morphology changes with female reproductive state in the mouth-brooding African cichlid *Astatotilapia burtoni*. *J Exp Biol* 220: 4463–4470.

Chu D, Stanton TK. 1998. Application of pulse compression techniques to broadband acoustic scattering by live individual zooplankton. *J Acoust Soc Am* 104: 39–55.

Demer DA, Andersen LN, Bassett C, Berger L, Chu D, Condiotty J, Cutter GR, et al. ICES Cooperative Research Report No. 336, 2017.

Derrick B, Toher D, White P. 2016. Why Welch's test is Type I error robust. *Quant Methods Psychol* 12: 30–38.

Gauthier S, Horne JK. 2004. Acoustic characteristics of forage fish species in the Gulf of Alaska and Bering Sea based on Kirchhoff-approximation models. *Can J Fish Aquat Sci* 61: 1839–1850.

Gorska N, Ona E, Korneliussen R. ICES CM documents No. 2004/R:18, 2004.

Grom K. 2015. Comparative anatomical study of swimbladder in different species of fish. *Sci Works Ser C Vet Med* 61: 156–160.

Kang D, Hwang D. 2003. *Ex situ* target strength of rockfish (*Sebastes schlegeli*) and red sea bream (*Pagrus major*) in the Northwest Pacific. *ICES J Mar Sci* 60: 538–543.

Korneliussen RJ (Ed.). ICES Cooperative Research Report No. 344, 2018.

Lundgren B, Nielsen JR. 2008. A method for the possible species discrimination of juvenile gadoids by broad-bandwidth backscattering spectra vs. angle of incidence. *ICES J Mar Sci* 65: 581–593.

Moore RH. 1970. Changes in the composition of the swimbladder gas of the striped mullet, Mugil cephalus, during hypoxia. *Comp Biochem Physiol* 34: 895–899.

Nakken O, Olsen K. 1977. Target strength measurements of fish. *Rapp. P.-v. Réun Cons Int Explor Mer* 170: 52–69.

Ostrovsky I, Goren M, Shapiro J, Snovsky G, Rynskiy A. Fish biology and ecology, in: T. Zohary, A. Sukenik, T. Berman, A. Nishri (Eds.), Lake Kinneret, Ecology and Management, Aquatic Ecology Series, Vol. 6., Springer, Dordrecht, 2014, pp. 273–292.

Cite this article as: Homma H, Ostrovsky I. 2021. The relationship between target strength frequency response and vertical swim velocity: a new approach for fish discrimination. *Aquat. Living Resour.* 34: 11